Characterization of thermally annealed tunnel junctions with preoxidized CoFe pinned electrode

Characterization of thermally annealed tunnel junctions with preoxidized CoFe pinned electrode

J. H. Lee, D. H. Im, C. S. Yoon, and C. K. Kim[a)]
Department of Materials Science and Engineering, Hanyang University, Seoul 133-791, Korea

Y. Ando, H. Kubota, and T. Miyazaki
Graduate School of Engineering, Tohoku University, Aoba-yama 05, Sendai 980-8579, Japan

Postannealed structure and electron transport properties of the magnetic tunnel junctions with preoxidized CoFe pinned electrode were compared with those of the conventional plasma oxidized junctions. The preoxidized junction exhibited its peak tunneling magnetoresistance ratio at 375 °C which is well above the optimal annealing of the normal junction. Using Auger electron spectroscopy and x-ray photoelectron spectroscopy of the thermally annealed junctions, structural and chemical changes after annealing were observed in the tunnel barrier as well as near the interface for both types of the junctions and these changes closely corresponded to the respective postannealed electrical properties. X-ray magnetic circular dichroism analysis indicated that the Co moment in the preoxidized CoFe electrode rose near the tunnel barrier/electrode interface as the optimal annealing temperature was reached. Our results demonstrated that the magnitude of spin polarized tunneling current is very sensitive to the interface structure and that any changes near the barrier interface during thermal annealing can greatly alter the electrical properties of the magnetic tunnel junctions. © 2003 American Institute of Physics. [DOI: 10.1063/1.1628827]

I. INTRODUCTION

Magnetic tunneling junctions (MTJs) relying on the spin-polarized electrons tunneling through a thin insulating layer have been actively studied because of their scientific significance and possible commercial application of the phenomenon in nonvolatile memory. Although earlier theories predicted the tunneling magnetoresistance (TMR) in these MTJs to be solely dependent on the spin polarization values of the ferromagnetic electrodes,[1] later experiments confirmed that the TMR effect was largely influenced by the nature of the tunnel barrier as well as the interfaces between the oxide barrier and ferromagnetic electrodes.[2] In fact, fabricating a reliable high-quality tunnel barrier has been the focus of the recent research in MTJs. The interplay between the TMR effect and the tunnel barrier becomes accentuated when the MTJs are thermally annealed due to the subtle changes in structural and electronic properties of the tunnel barrier during annealing. Interdiffusion near the barrier interfaces[3] and local structural changes in the barrier[4,5] have been identified affecting the postannealed properties of the MTJs. In addition, electrical properties of the MTJs after the thermal treatment are especially important since the integration of the tunnel junctions with the existing state-of-art semiconductor technology would require the magnetic junctions to withstand an annealing temperature above 300 °C.[6]

There has been intensive research efforts to improve the thermal stability of the MTJ, and it was recently shown that the thermal stability up to >400 °C can be achieved by modifying the electrode compositions.[7,8] In a previous study,

Ando *et al.* also showed that radical oxidation of the Al–oxide tunnel barrier greatly enhanced the thermal stability and demonstrated the structural differences between normal and radical oxidized junctions that led to the different postannealed behavior.[9] In this study, the work is further extended by pretreating the ferromagnetic electrode with oxygen prior to the plasma oxidation of the Al–oxide tunnel barrier and we show that the preoxidized junctions have nearly identical postannealed properties as the radical oxidized junctions. The annealed junctions were characterized using Auger electron spectroscopy (AES) and x-ray photoelectron spectroscopy (XPS) to demonstrate both structural and chemical changes occurring in the pretreated MTJ as well as in the normal junction. In addition, depth-resolved x-ray magnetic circular dichroism (XMCD) was employed to provide a direct evidence of changes in magnetic properties near the tunnel barrier during annealing.

II. EXPERIMENTAL PROCEDURE

The magnetic tunnel junctions were deposited by dc magnetron sputtering at room temperature. The stack structure consisted of $SiO_2/Ta(3\,nm)/Ni_{80}Fe_{20}(3\,nm)/Cu(20\,nm)/Ni_{80}Fe_{20}(3\,nm)/IrMn(10\,nm)/Co_{75}Fe_{25}(4\,nm)/Al(0.8\,nm)-oxide/Co_{75}Fe_{25}(4\,nm)/Ni_{80}Fe_{20}(20\,nm)/Ta(5\,nm)$, whose schematic structure is shown in Fig. 1. Details for preparation for the plasma oxidized junctions are detailed elsewhere.[9] For the preoxidized electrode samples, the $Co_{75}Fe_{25}(4\,nm)$ electrode was exposed to pure oxygen at 3×10^4 Pa for 10 min after which 0.8-nm-thick Al was deposited. Both normal and preoxidized samples were oxidized in plasma for 10 s.

[a)]Author to whom correspondence should be addressed; electronic mail: ckkim@hanyang.ac.kr
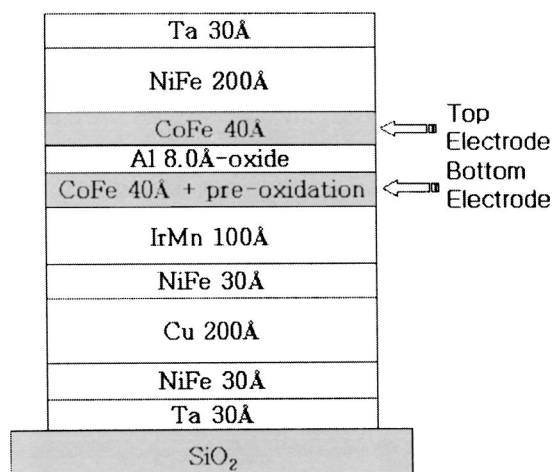
FIG. 1. Schematic diagram of the MTJ sample.

Thin film stacks were annealed at temperatures up to 425 °C under vacuum (10^{-6} Torr) for 1 h. Using Auger microprobe PHI680, the depth profiles were obtained with 2.5 keV/2.6 nA electron probe. Sputtering of the sample was achieved with 500 eV Ar ion beam at a sputtering rate of 10 Å/min and analyzed area was 2 μm$\times$3 μm. For XPS analysis, monochromatic x-ray generated from Al $K\alpha$ (15 kV) is used and sputteretching was done with Ar ion beam (1 kV, 45°). The sputtering rate was 6–7 Å/min. For the XMCD analysis, the experiment was performed at the BL-7A station in the Photon Factory (Japan) with 80% circularly polarized synchrotron x ray. The absorption spectra were obtained using a microchannel plate detector with -500 V electron retarding voltage in order to enhance the surface sensitivity.[10] Samples were sputtered in an UHV chamber with 1.5 kV Ar$^+$ ions. Magnetoresistance and I–V characteristics were measured by a four-probe method on junctions patterned by the photolithographic technique.

III. RESULTS AND DISCUSSION

Figure 2(a) shows the TMR ratio as a function of the annealing temperature for both normal and radical oxidized junctions which were both oxidized for 10 s to form the tunnel barrier. The normal junction exhibited typical postannealed behavior whereas the TMR ratio from the preoxidized junction showed a sharp rise in the TMR ratio at 375 °C. This is remarkably similar to the data previously obtained from the radical oxidized except for the slightly decreased the peak TMR ratio at 375 °C.[9]

In Figs. 2(b) and 2(c), the estimated barrier height and thickness are plotted as a function of the annealing temperature. Comparing with Fig. 2(a), the barrier height and thickness closely followed the TMR ratio graph. As seen in Fig. 2, the preoxidation of the bottom electrode surface led to completely different postannealed electron transport properties of the MTJ. It is speculated that excess oxygen at the bottom electrode/barrier interface was redistributed and more homogeneous oxide structure was formed during annealing. In the radical oxidation which exhibited similar postannealed properties as the preoxidized junctions, it was concluded that the
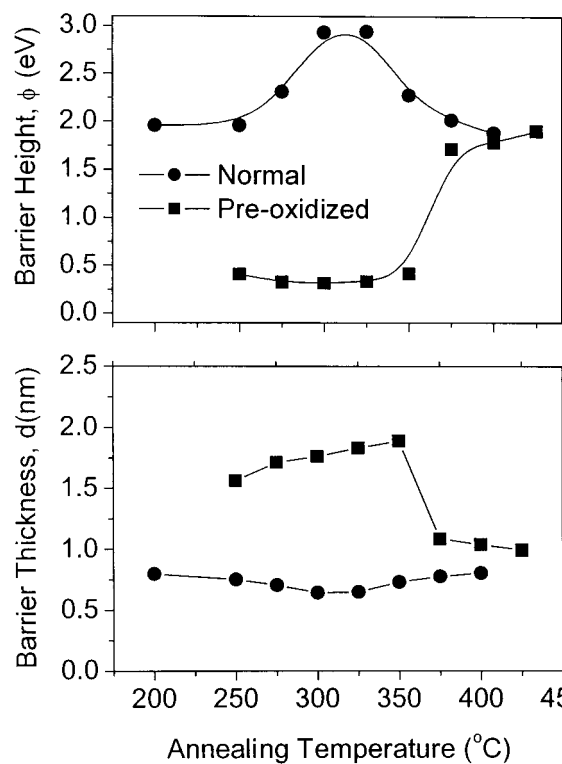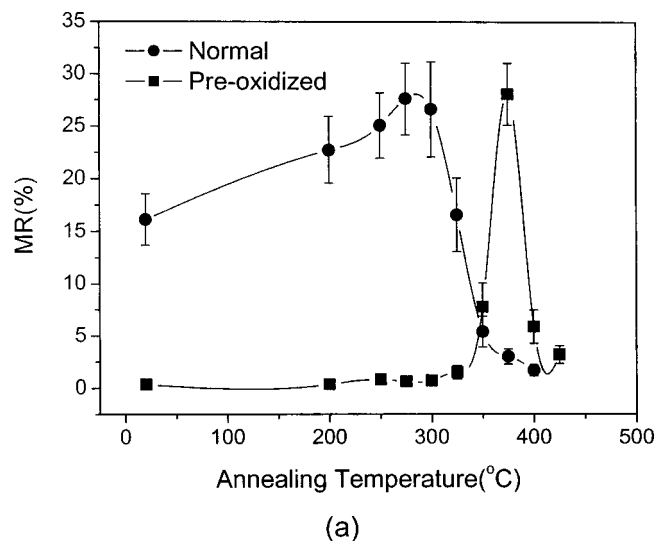

FIG. 2. (a) TMR ratio vs annealing temperature and (b) barrier height and thickness for the plasma (normal) and preoxidized junctions.

selective oxidation through the grain boundaries of the Al metal layer was realized by the radical oxidation, which resulted in the overoxidation of the bottom electrode surface, closely resembling the structure of the preoxidized junction.[9] The earlier result proves that the condition of the barrier interfaces plays a critical role in determining the magnitude of the spin polarized tunnel current.

Figure 3(a) shows the elemental concentration depth profiles obtained from the as-deposited junction with the plasma oxidized tunnel barrier. The asymmetric shape of the oxygen profile extending well into the CoFe and IrMn layers suggests that some oxygen were able to migrate into the
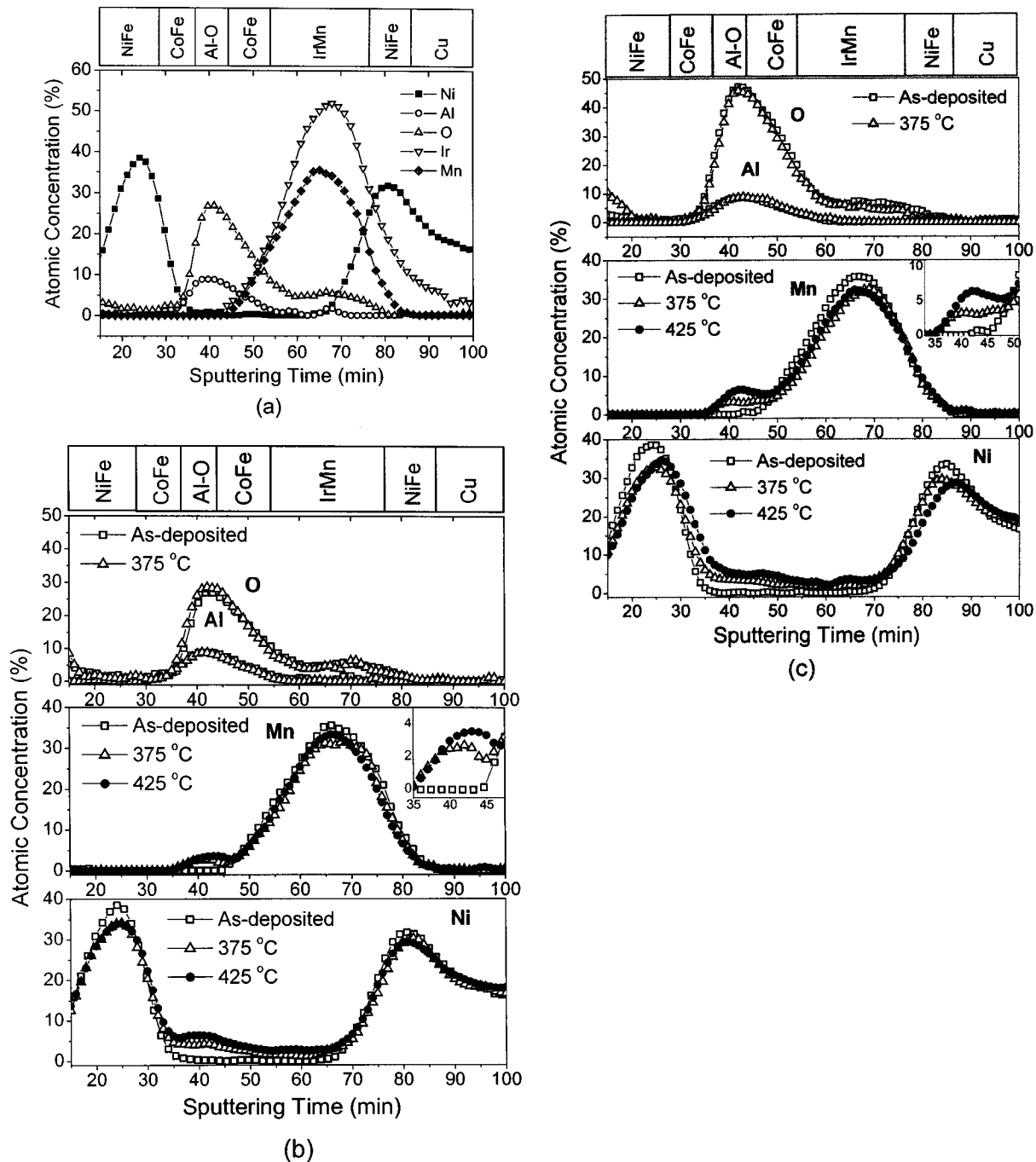
FIG. 3. Auger depth profiles: (a) as-deposited normal junction, (b) annealed normal junctions, and (c) annealed preoxidized junctions.

CoFe layer during deposition even prior to annealing. Figure 3(b) compares the Al, O, Mn, and Ni profiles from the normal junctions annealed at different temperatures. The concentration profiles for Al and O showed little change after annealing whereas diffusion of Mn and Ni was quite obvious. Diffusion of Mn, which proportionally increased in magnitude with increasing annealing temperature, was fully addressed elsewhere.[11] In the case of Ni, intermixing of Ni with the CoFe layer in the free electrode would reduce the spin polarization, thus deteriorating the TMR value of the junction.

In Fig. 3(c) are the depth profiles for the same set of elements from the preoxidized junctions annealed at different temperatures. Comparing the Al and O profiles in Figs. 3(b) and 3(c), the concentration ratio of O to Al for the preoxidized junction was much higher than that of the normal junction. The higher oxygen concentration of the preoxidized junction is likely due to the exposure of the CoFe layer to oxygen prior to the barrier deposition. Similar to the normal junction, annealing hardly altered the concentration profiles for Al and O while Mn and Ni readily diffused towards the oxide barrier in the preoxidized junctions. At 375 °C, a substantial degree of Mn diffusion towards the oxide barrier, as can be seen from the inset, was observed which is rather surprising because the preoxidized junction exhibited the peak TMR value at this temperature. The presence of Mn in

J. Appl. Phys., Vol. 94, No. 12, 15 December 2003

Lee *et al.* 7781

or near the tunnel barrier is believed to induce defect states and reduce the magnitude of spin polarized tunneling.[13] Figure 3(c), however, suggests that presence of Mn in the tunnel barrier may not be detrimental to the spin polarized tunneling. In fact, a similar conclusion was also drawn from the thermally stable MTJs prepared with FePt electrodes.[7]

Even though postannealed electron transport properties of the normal and preoxidized junctions vastly differed, no significant difference in the junction structure in response to thermal annealing were detected using AES spectroscopy. The AES data suggest that the structural change of the tunnel barrier is rather subtle or confined to a few atomic layers near the barrier/electrodes interfaces. In fact, neither did cross-sectional transmission electron microscopy show any gross changes in microstructure after annealing at 375 °C for the preoxidized junction.

XPS analysis was carried to probe the chemical states of Co, Fe, Mn, and Al near the tunnel barrier. As previously reported, the $Co \, 2P_{3/2}$ spectra near the barrier/bottom electrode interface for the normal junction retained the metallic peak shape and binding energy after annealing.[11] Similar XPS results were also observed in case of the preoxidized junctions, indicating that Co in the bottom electrode remained unoxidized in spite of the exposure to oxygen prior to the barrier formation.

In comparison, the Fe $3p$ spectra near the interface had an oxide peak for both normal and preoxidized junctions as indicated in Figs. 4(a) and 4(b). Since the Gibbs free energy of formation of the Fe–oxides (FeO: -245.6 kJ/mol, Fe_3O_4: -1018.0 kJ/mol, CoO: -216.5 kJ/mol, Co_3O_4: -763.25 at 298.15 K)[12] is higher than that of the Co–oxides, Fe would be oxidized in preference to Co in the CoFe electrode as reflected in the XPS data. For the normal junction, the Fe–oxide peak, however, disappeared at 275 °C at which the junction also exhibited the maximum TMR value. The same trend is also observed with the preoxidized junction for which the oxide peak disappeared at 375 °C, coinciding with the optimal annealing temperature for the junction. Recent theories and experiments indicated that the magnitude of the TMR is sensitive to the bonding state at the ferromagnet/oxide barrier; in fact, the sign of spin polarization can change depending on the electronic structure of the ferromagnet/insulator interface.[13] It was also shown that surface reconstruction of the barrier interface can also influence the magnitude of the spin polarized tunneling.[9] Here, our XPS data showed a rough correlation between the oxidation state of the ferromagnet near the interface and the magnitude of the TMR, further demonstrating the importance of the interface structure.

Examining the $Mn \, 2p_{3/2}$ spectra, it was found in all samples regardless of the annealing temperature that Mn was found near the interface in an oxide form. Meanwhile, the $Al \, 2p$ edge from the tunnel barrier for the preoxidized junction showed a subtle shift in binding energy when annealed at 375 °C as shown in Fig. 4(c) whereas the $Al \, 2p$ binding energy remained nearly constant for the normal junction. The binding energy shift in $Al \, 2p$ is related to the Fermi energy level change within the band gap[14,15] possibly caused by creation/removal of defects or the oxidation/reduction reac-
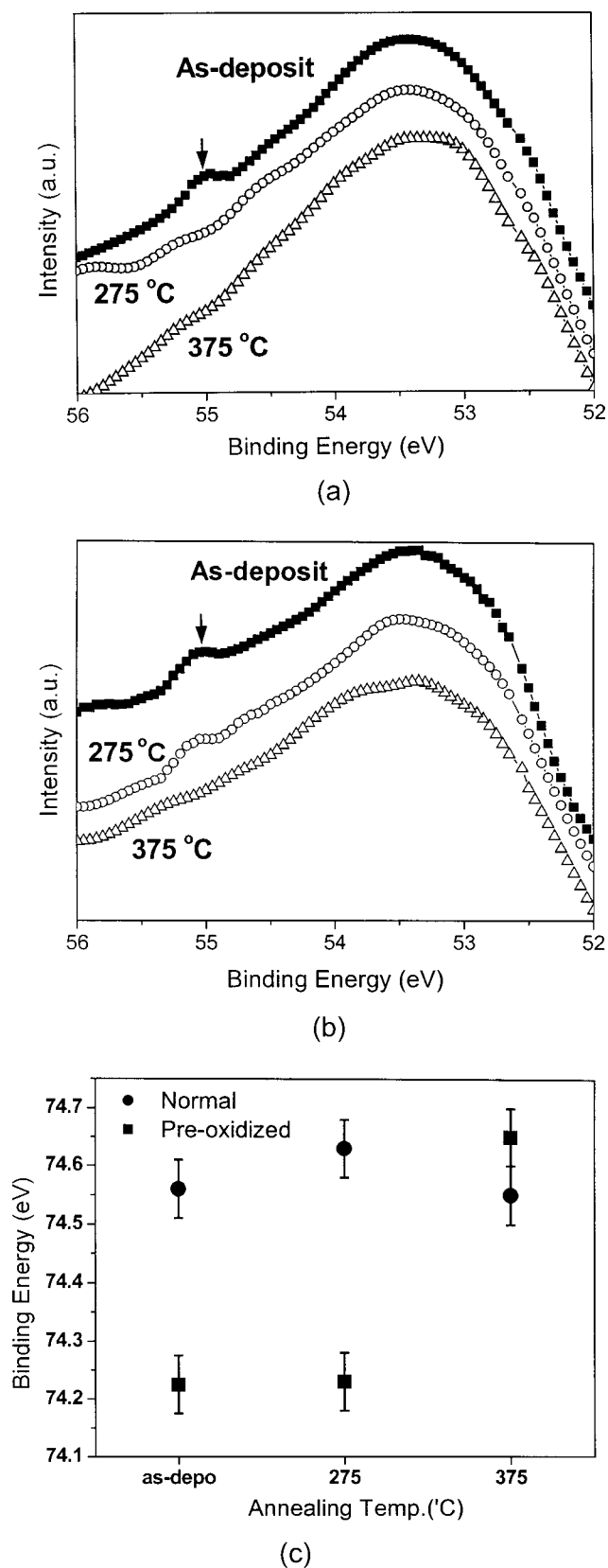

FIG. 4. (a) Fe $3p$ spectra obtained from the AlO_x/CoFe interface from the normal junctions annealed at different temperatures (the arrow indicate the oxide peak), (b) Fe $3p$ spectra obtained from the AlO_x/CoFe interface from the preoxidized junctions (the arrow indicate the oxide peak), and (c) binding energy of $Al \, 2p$ measured from the tunnel barrier from the annealed normal and preoxidized junctions.
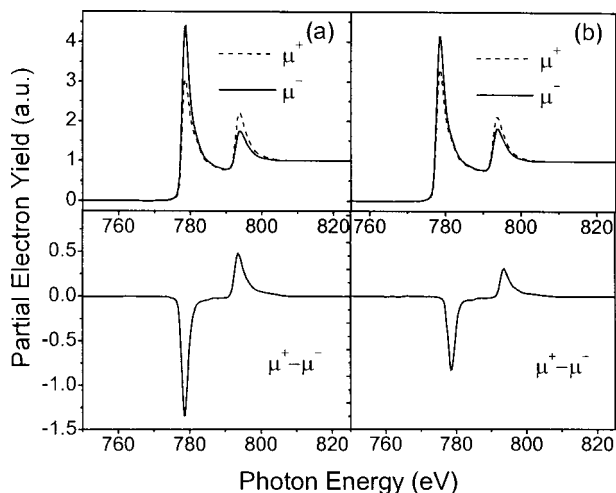
FIG. 5. Co 2*p* absorption spectra and calculated XMCD signal from the normal junctions annealed at 375 °C: (a) from the middle of the top CoFe electrode, and (b) near the oxide barrier.
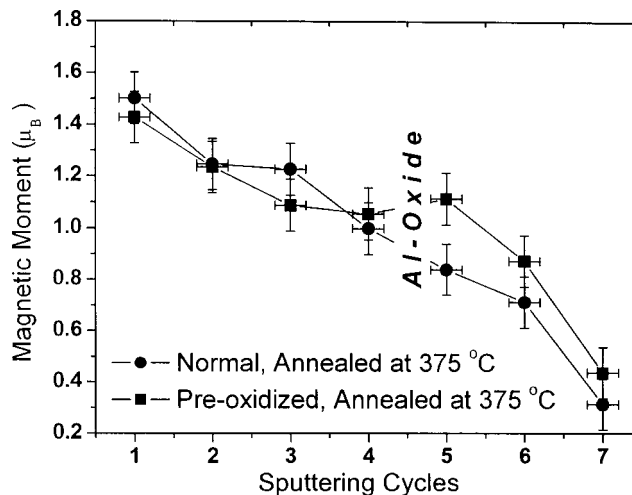
FIG. 6. Estimated magnetic moment (spin moment+orbital moment) from the XMCD depth profiles of the normal and preoxidized junctions. Each sputtering cycle removed ~0.8 nm of the material.

tions between the barrier oxide and Fe near the interface. XPS clearly shows that the tunnel junctions undergo structural changes during thermal annealing near the tunnel barrier and temperatures at which theses changes occur appears to strongly depend on the barrier interface.

Last, we used the XMCD analysis in order to estimate the magnetic moment of Co near the barrier interfaces. XMCD spectra were obtained using the microchannel detector plate which has relatively shallow probing depth compared to monitoring the sample drain current. Figure 5 shows the normalized Co XMCD spectra obtained from the middle of the top CoFe electrode and near the electrode/oxide barrier interface from the normal junction annealed at 375 °C. As can be seen, the intensity of the XMCD signal clearly decreased near the interface, suggesting the magnetization of Co dropped near the interface due to intermixing. This conclusion was, however, less clear when a full depth profile of the Co moment was calculated. The Co magnetic moment from the top and bottom electrodes is extracted from a series of XMCD signals obtained as a function of depth using the sum rule[16–18] and potted in Fig. 6. The first observation from the graph was that the Co moment decreased continuously past the Al–oxide barrier for both normal and preoxidized junctions when it is intuitively expected that the Co moment in the bottom electrode would rise away from the interface. Such a trend was observed in all the samples that were measured. We are not clear why the average Co moment of the bottom electrode is lower than that of the top electrode. It may be due to the effect of the antiferromagnetic IrMn layer lying under the bottom CoFe electrode whereas the CoFe top electrode is sandwiched between the NiFe and bottom CoFe layers which could provide some degree of ferromagnetic coupling. Comparing the Co moment from the two samples: normal and preoxidized junctions annealed at 375 °C, the Co magnetic moment from the preoxidized junction rose appreciably near the interface between the Al–oxide and the bottom electrode. Since maximum TMR was obtained at 375 °C for the preoxidized junction (~30%) whereas TMR for the normal junction dropped considerably at the same annealing

temperature, the relatively large Co moment measured near the interface for the preoxidized junction could be indicative of the optimal annealing temperature.

As demonstrated, the TMR junctions underwent both physical and chemical changes during thermal annealing. In addition, depending on the initial structure at the oxide barrier/bottom CoFe electrode interface, these changes occurred at different temperatures; thus, greatly altering the postannealed properties of the junction.

IV. CONCLUSION

We showed that the postannealed propertied of the TMR junctions can vastly differ depending on the initial structure at the oxide barrier/bottom CoFe electrode interface. Analyzing the thermally annealed TMR junctions using AES and XPS, both structural and chemical changes were observed in the tunnel barrier as well as near the interface and these changes closely corresponded to the postannealed properties of the junction. Although XMCD was employed to study the magnetic changes during annealing, the resulting data were not well understood. Further investigation is underway to better understand the changes in magnetic properties in the TMR junction during annealing.

ACKNOWLEDGMENTS

[1] M. Julliere, Phys. Lett. A **54**, 225 (1975).
[2] E. Y. Tsymbal, O. N. Mryasov, and P. R. LeClair, J. Phys.: Condens. Matter **15**, R109 (2003).
[3] S. Cardoso, P. P. Freitas, C. de Jesus, and J. C. Soares, J. Appl. Phys. **87**, 6058 (2000).

J. Appl. Phys., Vol. 94, No. 12, 15 December 2003

Lee *et al.* 7783

[4] J. H. Lee, H. D. Jeong, H. Kyung, C. S. Yoon, C. K. Kim, B. G. Park, and T. D. Lee, J. Appl. Phys. **91**, 217 (2002).

[5] Y. Ando, H. Kubota, M. Hayashi, M. Kamijo, K. Yaoita, C. C. Yu, X. F. Han, and T. Miyazaki, Jpn. J. Appl. Phys., Part 1 **39**, 5832 (2000).

[6] S. Tehrani, J. M. Slaughter, E. Chen, M. Durlam, J. Shi, and M. DeHerrera, IEEE Trans. Magn. **35**, 2814 (1999).

[7] N. Matsukawa, A. Odagawa, Y. Sugita, Y. Kawashima, Y. Morinaga, M. Satomi, M. Hiramoto, and J. Kuwata, Appl. Phys. Lett. **81**, 4784 (2002).

[8] X. Batlle, P. J. Cuadra, Z. Zhang, S. Cardoso, and P. P. Freitas, J. Magn. Magn. Mater. **261**, L305 (2003).

[9] Y. Ando, M. Hayashi, S. Iura, K. Yaoita, C. C. Yu, H. Kubota, and T. Miyazaki, J. Phys. D **35**, 2415 (2002).

[10] K. Amemiya, S. Kitagawa, D. Matsumura, T. Yokoyama, and T. Ohta, J. Phys.: Condens. Matter **15**, S561 (2003).

[11] C. S. Yoon, J. H. Lee, H. D. Jeong, C. K. Kim, J. H. Yuh, and R. Haasch, Appl. Phys. Lett. **80**, 3976 (2002).

[12] *The Oxide Handbook*, 2nd ed., edited by G. V. Samsonov (IFI/Plenum, New York, 1982), p. 45.

[13] E. Y. Tsymbal, I. I. Oleinik, and D. G. Pettifor, J. Appl. Phys. **87**, 5230 (2000).

[14] W. M. Mullins and B. L. Averbach, Surf. Sci. **206**, 52 (1988).

[15] L. P. H. Jeurgens, W. G. Sloof, F. D. Tichelaar, and E. J. Mittemeijer, Surf. Sci. **506**, 313 (2002).

[16] B. T. Thole, P. Carra, F. Sette, and G. van der Lann, Phys. Rev. Lett. **68**, 1943 (1992).

[17] P. Carra, B. T. Thole, M. Altarelli, and X. Wang, Phys. Rev. Lett. **70**, 694 (1993).

[18] C. T. Chen *et al.*, Phys. Rev. Lett. **75**, 152 (1995).